

Kolmogorov's Lagrangian similarity law newly assessed

Manuel Barjona¹ and Carlos B. da Silva^{1,*}

¹*Instituto Superior Técnico, Universidade de Lisboa,
Av. Rovisco Pais, 1049-001 Lisboa, Portugal.*

(Dated: March 10, 2022)

Abstract

Kolmogorov's similarity turbulence theory in a Lagrangian frame is assessed with new direct numerical simulations (DNS) of isotropic turbulence with and without hyperviscosity, which attain higher Reynolds numbers than previously available. It is demonstrated that hyperviscous simulations can be used to accurately predict second order Lagrangian velocity structure function (LVSF-2) in the inertial range. The results give strong support for Kolmogorov's Lagrangian similarity assumption and allow to compute the universal constant of the LVSF-2, which gives $C_0 = 7.5 \pm 0.2$, with a new level of confidence.

* carlos.silva@tecnico.ulisboa.pt

Introduction. Turbulence arises in the motion of fluids and plasmas and is crucial for a range of diverse problems in astrophysics, geophysics, biology, and engineering. Almost all the existing body of knowledge on turbulence is linked to the celebrated *similarity theory* of Kolmogorov[1, 2], which can predict the statistics of the velocity field $u_i(\vec{x}, t)$ at fixed positions \vec{x} (Eulerian frame).

When the turbulent motion is responsible for the transport of particles a Lagrangian similarity theory is usually invoked[2, 3], which is used to predict many aspects of cloud formation, combustion, pollutant dispersion and planet formation [4]. It is therefore surprising that, in contrast with the Eulerian similarity theory, even the most basic results from Kolmogorov's Lagrangian similarity theory have not yet been confirmed by either numerical simulations or experimental data [5].

The key variable of interest here is the n^{th} -order Lagrangian velocity structure function (LVSF-n),

$$D_L^n(\tau) = \overline{[\delta u_i(\tau)]^n}, \quad (1)$$

where $\delta u_i(\tau) = u_i(\vec{x}_0, t + \tau) - u_i(\vec{x}_0, t)$ is the velocity increment along a particle trajectory, \vec{x}_0 is the initial particle position, t is a given time instant, τ is the elapsed time, and the line ' $\overline{}$ ' represents an averaging operation. Statistical stationarity and isotropy imply that the probability density functions (PDF) of δu_i ($i = 1, 2, 3$) are equal and independent of \vec{x}_0 and t , and $\overline{u_i} = 0$.

The Lagrangian similarity theory makes exact predictions for the LVSF-n, for time lags within an 'inertial range region' such that $\tau_\eta \ll \tau \ll \tau_L$, where $\tau_\eta = (2s_{ij}s_{ij})^{-1/2}$ is the Kolmogorov time, and $s_{ij} = (\partial u_i/\partial x_j + \partial u_j/\partial x_i)/2$ is the strain rate tensor, while $\tau_L = \int_0^\infty \rho(\tau) d\tau$ is a Lagrangian integral time, where $\rho(\tau) = \overline{u_i(t+\tau)u_i(t)}/3\overline{u_i^2}$ is the auto-correlation velocity function. Specifically, it predicts that $D_L^n(\tau) \sim \tau^{\xi_n}$, where the scaling exponent is $\xi_n = n/2$. In particular, for the LVSF-2 self-similarity yields,

$$D_L^2(\tau) = C_0 \varepsilon \tau, \quad (2)$$

where C_0 is a universal constant, $\varepsilon = 2\nu s_{ij}s_{ij}$, is the dissipation rate, and ν is the kinematic viscosity. This law is believed to be universal because it is linear in ε and thus no intermittency corrections are required.

Until now, and after decades of research, numerical or experimental verification of Eq. (2) has proven elusive. The importance of this law cannot be overemphasised, as it make

the basis of virtually all the computations routinely used for turbulent particle transport predictions [4]. It is generally believed that this difficulty is due to the lack of existing experimental and numerical data with sufficient accuracy at sufficiently high Reynolds numbers, since the existence of a range with $\tau_\eta \ll \tau \ll \tau_L$, strongly depends on having data at high Reynolds numbers, which is very difficult to obtain.

In the present work we carry out new (newtonian and hyperviscous) direct numerical simulations (DNS), at much higher Reynolds numbers than before, and we demonstrate that the hyperviscous simulations can be used to accurately predict the inertial range scaling laws of the LVSF-2. The new simulations, together with a novel analysis of the LVSF-2 allow us to present strong new evidences in support of Kolmogorov's Lagrangian similarity theory, and to definitely establish the value of the universal constant C_0 .

Direct numerical simulations. Several DNS of statistically stationary (forced) isotropic turbulence in a periodic box with sizes 2π including point particles (tracers), were carried out using a classical pseudo-spectral code, previously used in [6, 7], to numerically integrate the hyperviscous Navier-Stokes equations [8–10],

$$\frac{\partial u_i}{\partial t} + u_j \frac{\partial u_i}{\partial x_j} = -\frac{1}{\rho} \frac{\partial p}{\partial x_i} + (-1)^{h+1} \nu_h \Delta^h u_i + f_i, \quad (3)$$

where u_i and p are the velocity and pressure fields, respectively, while f_i is an artificial forcing, which is uncorrelated with the velocity field and delta-correlated in time[6]. In all the simulations the total power input forcing P , which on average equals the viscous dissipation rate $P = \varepsilon$, is equal to $P = 10 \text{ (m}^2\text{s}^{-3}\text{)}$, and the forcing is imposed on the first 2 wavenumbers, and is concentrated in wavenumber $k_f = 2$. h is the order of the hyperviscosity and ν_h is the corresponding hyperviscosity (ρ is the fluid density). The Navier-Stokes equations are recovered for $h = 1$, while $h \neq 1$ corresponds to the hyperviscous simulations. Table I summarises the DNS used in this work. The number of tracked particles N_p increases with N , attaining $N_p = 1, 2$ million tracers for the biggest DNS. The particles tracking uses the same (3rd-order) Runge-Kutta time-stepping scheme used in the Eulerian DNS [6], and a cubic interpolation is used to interpolate the velocity into the particle positions. Full details are given in [11].

A set of 6 Navier-Stokes DNS ($h = 1$) were carried out with Reynolds numbers of up to $Re_\lambda = 381$ and resolutions of $k_{max}\eta \approx 1.6$, essentially to demonstrate that hyperviscosity

TABLE I. Parameters of the DNS without ($h = 1$) and with ($h = 8$) hyperviscosity (left and right sides of the table, respectively): Number of grid points (N^3); Reynolds number based on the Taylor micro-scale (Re_λ); Kinematic viscosity (ν); Ratio between the integral and Kolmogorov time scales (τ_L/τ_η); Resolution ($k_{max}\eta$); Wavenumber corresponding to the maximum enstrophy in the hyperviscous simulations (k_d); Location of the peak maximum of $D_L^2(\tau)$ (τ_0^*); Maximum of $D_L^2(\tau)/(\varepsilon\tau)$ (C_0^*); Location of the inertial range peak maximum of $\zeta_2'(\tau)$ (C_0^{**}); $\zeta_2(\tau)$ for $\tau = \tau_0^{**}$ (α); Universal constant of the LVSL-2 computed through Eq. (10) (C_0^{**}).

N^3	Re_λ	ν	τ_L/τ_η	$k_{max}\eta$	τ_0^*/τ_η	C_0^*	τ_0^{**}/τ_η	α	C_0^{**}	N^3	Re_λ	τ_L/τ_η	k_d	τ_0^*/τ_η	C_0^*	τ_0^{**}/τ_η	α	C_0^{**}
32^3	24	0.1	3.4	1.6	3.7	2.0	—	—	—	128^3	276	13.5	24	4.0	5.2	—	—	—
64^3	50	0.04	5.2	1.6	3.8	3.0	—	—	—	256^3	450	22.1	54	4.3	5.7	9.0	0.82	7.8
128^3	88	0.015	7.7	1.5	4.0	4.0	—	—	—	512^3	701	35.9	105	4.4	6.0	9.0	0.88	7.4
256^3	131	0.0071	12.2	1.8	4.2	4.4	—	—	—	1024^3	1102	49.1	207	4.7	6.3	9.0	0.91	7.4
512^3	228	0.0025	17.7	1.6	4.4	5.1	10.5	0.78	7.7	2048^3	1744	88.7	412	4.9	6.6	9.0	0.92	7.6
1024^3	381	0.001	30.8	1.6	5.2	5.7	10.5	0.86	7.4									

does not affect the Lagrangian statistics in the inertial range. A total of 5 hiperviscous DNS was carried out with $h = 8$, and a hyperviscosity obeying the relation $\nu_h (N/2)^{2h} \Delta t \approx 0.5$, where Δt is the time step of the simulations [8, 9]. The Reynolds numbers of the hyperviscous DNS is given by $Re_\lambda = C_8(k_d/k_f)^{\frac{2}{3}}$, where $C_8 = 50$ and k_d is the peak enstrophy wavenumber.

Lagrangian statistics from hyperviscous simulations. By concentrating the viscous dissipation on a small range of high wavenumbers near the maximum k_{max} , hyperviscous simulations substantially increase the extent of the inertial range region compared to 'Newtonian' ($h = 1$) DNS, which allows to attain much higher Reynolds numbers [8–10]. Recently, hyperviscous simulations were used to study the shape of the energy spectrum in viscoelastic turbulence [7], and here we show that this technique can be used to study in detail the Lagrangian statistics of turbulence for inertial times $\tau_\eta \ll t \ll \tau_L$. The realisation that hyperviscosity can be used to study the Lagrangian statistics in the inertial range is an innovative aspect

of the present work, which should not be surprising. Recall that in virtually all similar DNS studies the large scales are also forced, and thus are not an exact solution of the Navier-Stokes equations, however this does not prevent the study of turbulence statistics in the inertial range.

Table I shows that the hyperviscous DNS with 2048^3 grid points attains a Reynolds number of $Re_\lambda \approx 1700$, which is much higher than in previous numerical works [5, 12], and, as we will see below, allows for the first time to directly observe the Lagrangian Kolmogorov similarity. Specifically, extensive validation tests have shown that for $\tau_\eta \ll t \ll \tau_L$, Lagrangian statistics from Navier-Stokes ($h = 1$) and hyperviscous ($h = 8$) simulations at the same Reynolds number are virtually equal. Figures 1 (a-d) display several of these results while other tests are described in [11].

Figure 1 (a) shows the Lagrangian correlation function $\rho(\tau)$ for the velocity components (u, v, w) in the Newtonian and hyperviscous simulations corresponding to $N^3 = 256^3$. The agreement between the Newtonian and hyperviscous results is very good, and moreover all the correlations exhibit a clear exponential decay as predicted in [13]. Furthermore, $\rho(\tau)$ obtained for u , v , and w is very similar which shows that the forcing does not impose any significative level of anisotropy in the present simulations.

Figure 1 (b) shows $D_L^2(\tau)$ normalised by $\varepsilon\tau$, obtained with Newtonian and hyperviscous simulations, for increasing Reynolds numbers. First, in both cases a slope of $+1$ is obtained in the interval $\tau < \tau_\eta$ as expected [13] (see also Fig. 2). Secondly, for $\tau > \tau_L$ a slope of -1 is recovered, again as expected since $\rho(\tau)$ vanishes. Thirdly, the peak value (C_0^*) increases with the Reynolds number, regardless of whether the simulations are Newtonian or hyperviscous. Finally, the exact location of the peaks (τ_0^*) also shows the consistency of the hyperviscous results *i.e.* the Newtonian simulations this peak occurs at a time lag τ_0^* , which is slightly higher than in the hyperviscous simulations, but since this peak is in the transition between the dissipative and integral time scales the slight smaller location of the peak in the hyperviscous simulation is actually consistent with the decrease of the width of the dissipative length scales in these simulations.

The definitive demonstration that hyperviscous simulations can accurately predict the Lagrangian statistics at inertial time lags is shown in the next two figures. Figure 1 (c) shows the constant C_0 defined in Eq. (2) for the Newtonian and hyperviscous simulations, as function of Reynolds number, for $Re_\lambda \leq 800$, together with the empirical relation $C_0^* =$

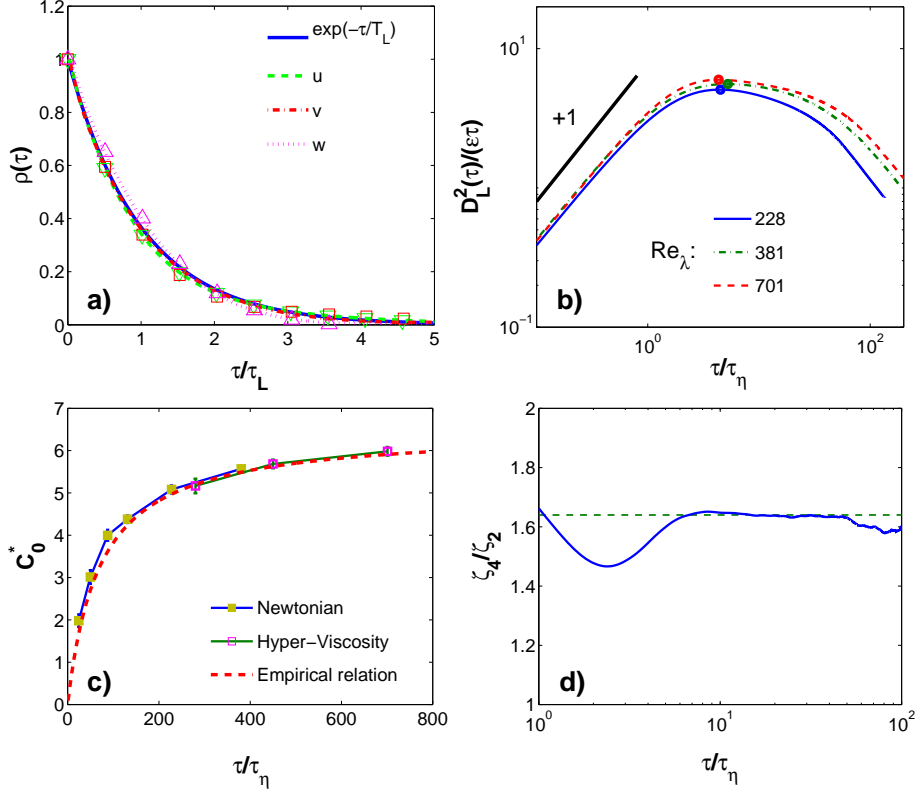


FIG. 1. (a) Lagrangian correlation function for $u_i = (u, v, w)$ for the Newtonian (symbols) and hyperviscous (lines) DNS with $N^3 = 256^3$. The function $e^{-\tau/\tau_L}$ is also added for comparison; (b) Normalised LVSF-2 for some Newtonian and Hyperviscous simulations listed in table I at increasing Reynolds numbers; (c) Evolution of the peak value C_0 defined in Eq. (2) as function of Reynolds number, for several Newtonian and hyperviscous simulations, compared with the empirical relation $C_0^* = 6.5/(1 + 70/Re_\lambda)$, from [12]. (d) Scaling coefficient of the LVSF-4 (ζ_4) obtained from the hyperviscous simulation with $N^3 = 1024^3$ ($Re_\lambda = 1102$). The green dashed line has the constant value of 1.66.

$6.5/(1 + 70/Re_\lambda)$ from [12], which is used here only to compare the present results with C_0 obtained in previous numerical simulations. It is clear that C_0 computed from the Newtonian and hyperviscous simulations are virtually equal for the same Reynolds number. Moreover, the presents values of C_0 have excellent agreement with previous numerical simulations.

Finally, figure 1 (d) shows the scaling coefficient ζ_4/ζ_2 from the extended similarity theory[14], where $\zeta_n = d[\log D_L^n(\tau)]/d[\log D_L^2(\tau)]$, for the hyperviscous simulation with $N^3 = 1024^3$ ($Re_\lambda = 1102$), as function of the time lag (note that $\zeta_2 = 1$). Recall that

the this expression allows the computation of inertial scaling coefficients even in the absence of an extensive inertia range. ζ_4 was averaged in the interval $10 \leq \tau/\tau_\eta \leq 40$, and the uncertainty estimate of the scaling coefficient uses the maximum difference between ζ_4 computed with the mean value of the (u, v, w) velocity components, and ζ_4^i computed using only the i -th velocity component. For inertial range times ζ_4 is approximately constant, $\zeta_4 = 1.64 \pm 0.03$, and has excellent agreement with the value obtained by Benzi *et al.* [14] using the extended self-similarity concept [15], where $\zeta_4 = 1.66 \pm 0.02$. It is noteworthy that hyperviscous ζ_4 is precisely inside the interval predicted by the multifractal formalism [14].

The remarkable agreement between the Lagrangian statistics from Newtonian and hyperviscous simulations, for inertial time lags, allows us to use hyperviscous simulations to study the Lagrangian self-similarity in turbulent flows, as discussed below.

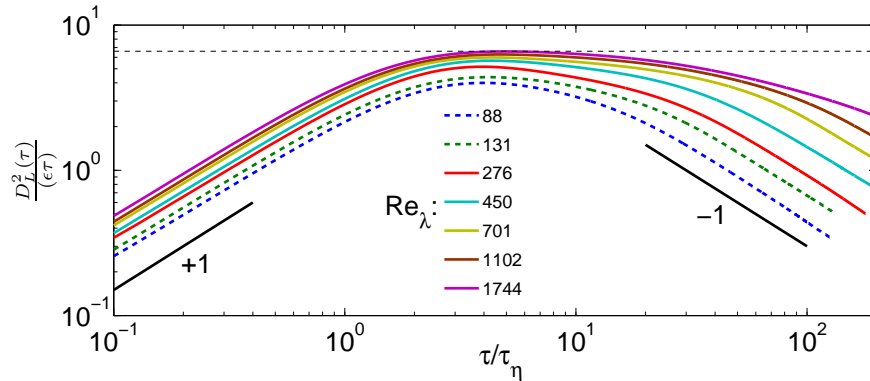


FIG. 2. Lagrangian velocity structure function of order 2 (LVSF-2), normalised by $\varepsilon\tau$, as function of the time lag τ for several Reynolds numbers from the Newtonian and hyperviscous simulations (listed in table I). The horizontal dashed line is at $C_0 = 6.6$.

Self-similarity of the Lagrangian 2nd order structure function. The new DNS were used to assess whether the 2nd order Lagrangian velocity structure function (LVSF-2) obeys the Lagrangian self-similarity relation predicted by Kolmogorov in the form of Eq. (2). The Reynolds numbers attained in the biggest of these simulations is $Re_\lambda \approx 1700$, which is much higher than previously available [5].

In order to prove the Lagrangian self-similarity two conditions have to be fulfilled: *i)* $D_L^2(\tau)$ normalised by $\varepsilon\tau$ must display a plateau, with a universal constant $C_0 = D_L^2(\tau)/(\varepsilon\tau)$ and, *ii)* the same constant must be observed for the three (3) velocity components, since

small scale isotropy is assumed. Figure 2 shows the LVSF-2 as function of the time lag τ in logarithmic coordinates, for several Reynolds numbers/simulations.

As the Reynolds number increases the function $D_L^2(\tau)/(\epsilon\tau)$ clearly tends to a constant value $C_0 \approx 6.6$. Specifically, for the simulation with $Re_\lambda = 1744$ the observed plateau, where $D_L^2(\tau)/\epsilon\tau \geq 0.99C_0^*$, is observed for $3.8 \lesssim \tau/\tau_\eta \lesssim 7.0$, which is about 27% of a decade in τ/τ_η . It is possible to see that after the peak value $D_L^2(\tau)/\epsilon\tau$ at $\tau/\tau_\eta \approx 4$, there is a region between $5 \lesssim \tau/\tau_\eta \lesssim 30 - 80$ (higher upper limits for higher Reynolds numbers), where a new slope, less steeper than -1 , is observed. It is clear that this secondary slope tends to ≈ 0 (plateau) as the Reynolds number increases, an interesting feature that had not yet been observed before.

The second requirement was assessed by analysing the values of the parameter $e = \frac{\max(|C_0^* - C_0^i|)}{C_0^*}$. Stronger isotropy is recovered for the higher Reynolds numbers cases with $e = 0.013, 0.011$ and 0.003 , for the simulations with $Re_\lambda = 701, 1102$ and 1744 , respectively, which shows that isotropy has been recovered in the present simulations, and attests that one of the basic assumptions of Kolmogorov's Lagrangian self-similarity is indeed observed here.

The results from the high Reynolds numbers obtained with the new hyperviscous DNS can be used also to refine the empirical laws previously obtained for C_0^* . In reference [12] the data available by then was used to determine the coefficients a and b for a scaling curve with the form,

$$C_0^* = a / (1 + b/Re_\lambda), \quad (4)$$

where in that case the values of $a = 6.5$ and $b = 70$ were obtained. Considering a similar curve for the present data we obtain $a = 6.9$ and $b = 1.97$, for an error of $e = 0.0026$. Figure 3 shows the comparison of the two curves where one can foresee that the present data suggests that the asymptotic value of C_0^* is clearly higher than previously thought [12]. We also considered adjusting the present data to a curve of the form,

$$C_0^* = c / (1 + d/Re_\lambda^{1/2}), \quad (5)$$

where constant values of $c = 7.8$ and $d = 8.0$ are obtained for yet a smaller error, namely $e = 0.00092$. Given the input from higher Reynolds numbers and the small associated error Eq. (5) can be considered to be the best approximation for C_0^* in existence.

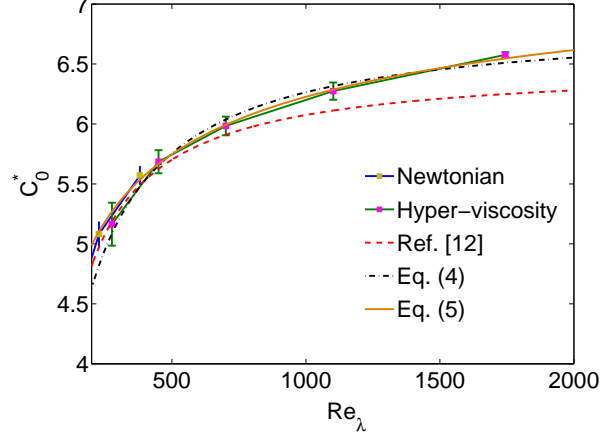


FIG. 3. LVSF-2 constant C_0 , obtained from the new hyperviscous simulations (listed in table I) compared with the empirical relation (Eq. 4) from [12], and new empirical curves obtained with the present new data using Eqs. (4) and (5), respectively.

The previous results show that the LVSF-2 nearly exhibits the predicted inertial range plateau to a degree not previously observed, however they do not allow one to finally establish the value of the universal constant C_0 , unless one is prepared to risk something as crude as extrapolating the data using Eq. (5). There are however, a couple of interesting observations that one can gather from a close inspection of the LVSF-2, that shed new light on this challenging old problem.

To describe these observations Figs. 4 (a-d) shows the LVSF-2 and its (logarithmic) first and second derivatives defined as,

$$\zeta_2(\tau) = \frac{d(\log(D_L^2(\tau)))}{d(\log(\tau))}, \quad (6)$$

and,

$$\zeta_2'(\tau) = \frac{d^2(\log(D_L^2(\tau)))}{d^2(\log(\tau))}, \quad (7)$$

respectively.

Already when $D_L^2(\tau)$ is normalised by $2u'^2$ (Fig. 4 a) we see the emergence of three different power law regions, associated with the dissipative (+2), inertial (+1), and large (0) time scales, however we can more clearly observe the emergence of the inertial range plateau by analysing the first derivative $\zeta_2(\tau)$ which is shown in Figs. 4 (b-hyperviscous, c-Newtonian).

The curves show a characteristic change of shape around $\tau \approx 10\tau_\eta$ for all simulations, and

interestingly, the slope of $\zeta_2(\tau)$ following this point tends to decrease as the Reynolds number increases, indicating a tendency for a plateau. Notice that the point where this happens (which we name τ_0^{**}), being one order of magnitude larger than τ_η , is certainly more likely to carry information regarding the inertial time scales than the point near $\tau_0^* \approx 4\tau_\eta$, typically used to assess C_0^* , where the viscous effects are still surely felt. The inertial range plateau in $D_L^2(\tau)$, if it exists, will be easily observed in $\zeta_2(\tau)$ through a range of values of τ where $\zeta_2(\tau) \approx 1$.

Finally, the second derivative of $D_L^2(\tau)$, $\zeta_2'(\tau)$, is shown in Fig. 4 (d) for the hyperviscous simulations. One can see that all the curves display a peak near $\zeta_2'(\tau) \approx 0$ at $\tau = \tau_0^{**}$, and the inertial range plateau in $D_L^2(\tau)$, if it exists, would be observed as a range of values of τ where $\zeta_2'(\tau) = 0$. We now rigorously define τ_0^{**} as the location of this peak in all the simulations. Table I lists the values of τ_0^{**} obtained for the higher Reynolds numbers. Due to some 'noise' in the statistical convergence around τ_0^{**} the value of τ_0^{**} used here is obtained with a window of width equal to $1\tau_\eta$ *i.e.* we chose data in a small interval with $[-0.5 \leq \tau/\tau_\eta \leq 0.5]$ centred around τ_0^* to compute this value.

Using the observations made above we are finally in condition to compute the value of the universal constant C_0 , directly from our data. We define a power α such that one can write,

$$D_L^2(\tau) = C_0 \epsilon \tau \left(\frac{\tau}{\tau_\eta} \right)^{\alpha-1}. \quad (8)$$

With this definition it follows from Kolmogorov's Lagrangian similarity that for inertial range time lags $\tau_\eta \ll \tau \ll \tau_L$ and in the asymptotic limit of infinite Reynolds numbers, $\alpha \rightarrow 1$. We now note, from the discussion of Figs. 4 (a-d), that this asymptotic result is concomitant with $\zeta_2(\tau_0^{**}) \rightarrow 1$, so that, in this limit ($Re_\lambda \rightarrow \infty$) one can write,

$$\alpha = \zeta_2(\tau_0^{**}), \quad (9)$$

and therefore the universal constant C_0 can be computed through,

$$C_0^{**} = \frac{D_L^2(\tau)}{(\epsilon \tau)} \left(\frac{\tau}{\tau_\eta} \right)^{1-\alpha}, \quad (10)$$

in the limit of $Re_\lambda \rightarrow \infty$ for $\tau_\eta \ll \tau \ll \tau_L$.

Figure 5 shows C_0^{**} computed with Eq. (10), for the higher Reynolds simulations used in the present work (Newtonian and hyperviscous). It is clear that an inertial range is

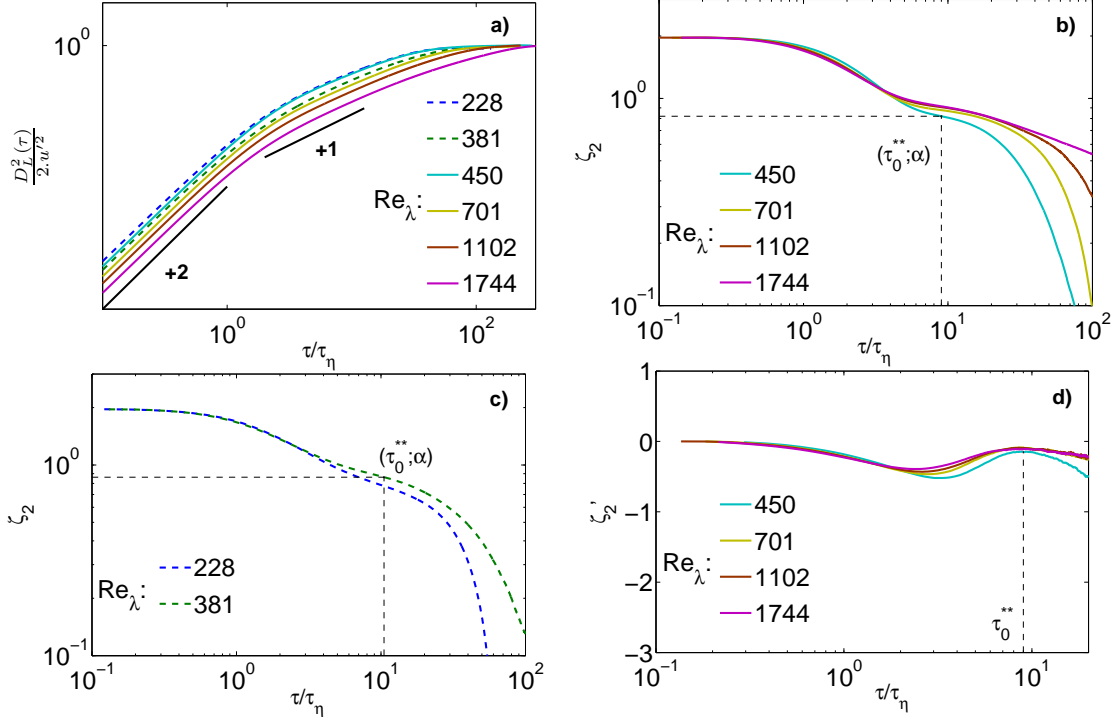


FIG. 4. Second order Lagrangian velocity structure function, $D_L^2(\tau)$ (a), and its first ζ_2 (b-hyperviscous, c-Newtonian), and second ζ_2' (d), (logarithmic) derivatives, as function of the time lag τ , for all the higher Reynolds simulations used in the present work.

observed since all the curves collapse for time lags near τ_0^{**} . Specifically, the width of the inertial range plateau *i.e.* the interval of time lags in which Eq. (10) is greater than 99% of its peak value, is tremendously increased here compared to the plateau associated with $C_0^* = D_L^2(\tau_0^*)/(\varepsilon\tau_0^*)$, which is obvious when comparing Figs. 2 and 5.

We now define $\alpha = \zeta_2(\tau_0^{**})$ for all our (finite Reynolds number) simulations, thereby extending the definition in Eq. (9). Table I displays the values of α for the higher Reynolds number simulations, where the associated possible variation (due to the window used to obtain τ_0^{**} described above) is equal to ± 0.01 . It is noteworthy that α computed using Eq. (9), is precisely the value that maximizes the width of the inertial range plateau. Furthermore, we note that as the Reynolds number increases $\tau_0^* \rightarrow \tau_0^{**}$, which further supports the fact that τ_0^{**} rather than τ_0^* should be used to obtain C_0 .

Finally, we compute C_0^{**} through Eq. (10) and we obtain $C_0^{**} = 7.5 \pm 0.2$ for all the higher Reynolds simulations (see also table I). Interestingly, if one uses Eq. (5) to estimate the asymptotic value of the Reynolds number that would lead to $C_0^* = 7.5$ we obtain

$Re_\lambda \approx 38,000$. This value is not far from the typical value of $Re_\lambda \approx 30,000$ estimated as the asymptotic Reynolds number needed to obtain C_0^* that has been predicted in some references *e.g.* [5]. Furthermore, we see that the value of $C_0 = 7.2$ obtained in that paper is also consistent with the present results.

Even though the present results cannot definitely prove Kolmogorov's Lagrangian similarity, in particular regarding the LVSF-2, they certainly provide a stronger support for its validity than had been observed thus far, and allow the computation of the universal constant C_0 with a new degree of certainty.

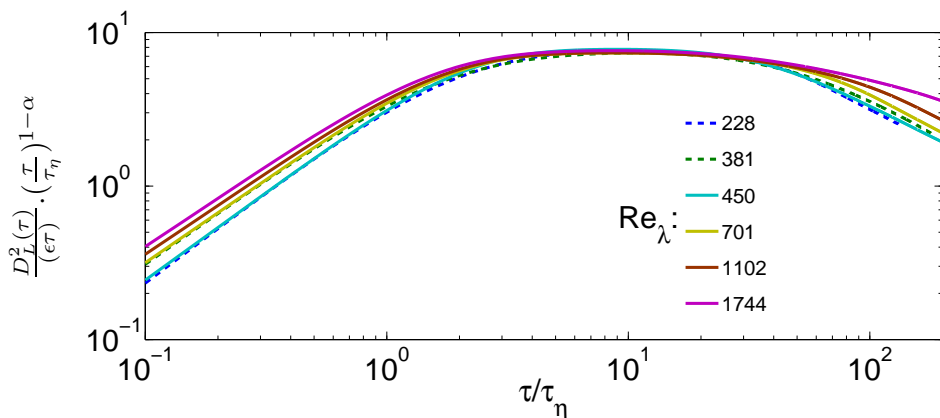


FIG. 5. Constant C_0^{**} obtained from Eq. (10) for all the simulations used in the present work. A constant value of $C_0^{**} = 7.5 \pm 0.2$ is observed for inertial range time lags.

Conclusions. New Newtonian and hyperviscous direct numerical simulations (DNS) transporting millions of tracers were carried to analyse the second order Lagrangian velocity structure function (LVSF-2). The new hyperviscous DNS attain a Reynolds number of $Re_\lambda \approx 1700$, which is the highest Reynolds number attained so far in numerical investigations of Lagrangian turbulence, and it is shown that these hyperviscous simulations can be used to accurately compute the LVSF-2 for inertial range time lags. The new results shown an unprecedented strong support for Kolmogorov's similarity turbulence theory in a Lagrangian frame, and the universal constant defined in the LVSF-2 is computed with a new degree of confidence, giving $C_0 = 7.5 \pm 0.2$.

Acknowledgements. We acknowledge PRACE for awarding us access to resource Marenos-

trum III based in Spain at <https://www.bsc.es>.

- [1] A. N. Kolmogorov, “Local structure of turbulence in an incompressible fluid for very large Reynolds numbers,” *Dokl. Akad. Nauk SSSR* **30**, 301 (1941).
- [2] A. S. Monin and A. M. Yaglom, *Statistical fluid mechanics: mechanics of turbulence, Vol. 2* (M.I.T. Press, Cambridge., 1975).
- [3] G. Falkovich, K. Gawedzki, and M. Vergassola, “Particles and fields in fluid turbulence,” *Rev. Mod. Phys.* **73**, 913 (2001).
- [4] P. A. Davidson, Y. Kaneda, and K. Sreenivasan, *Ten Chapters of Turbulence* (Cambridge University Press, 2013).
- [5] B. L. Sawford and P. K. Yeung, “Kolmogorov similarity scaling for one-particle lagrangian statistics,” *Physics of Fluids* **23**, 091704 (2011).
- [6] P. C. Valente, da C. B. da Silva, and F. T. Pinho, “The effect of viscoelasticity on the turbulent kinetic cascade,” *J. Fluid. Mech.* **760**, 39 (2014).
- [7] P. C. Valente, da C. B. da Silva, and F. T. Pinho, “Energy spectra in elasto-inertial turbulence,” *Phys. Fluids* **28**, 075108 (2016).
- [8] V. Borue and S. A. Orszag, “Forced three-dimensional homogeneous turbulence with hyperviscosity,” *Europhysics Letters* **29**, 687 (1995).
- [9] V. de Borue and S. Orszag, “Local energy flux and subgrid-scale statistics in three dimensional turbulence,” *J. Fluid Mech.* **366**, 1 (1998).
- [10] A. G. Lamorgese, D. A. Caughey, and S. B. Pope, “Direct numerical simulation of homogeneous turbulence with hyperviscosity,” *Physics of Fluids* **17** (2005).
- [11] M. Barjona, “Lagrangian statistics in homogeneous isotropic turbulence: Newtonian and hyperviscous fluids,” MSc thesis, Instituto Superior Técnico (2016).
- [12] B. Sawford, P. K. Yeung, and J. Hackl, “Reynolds number dependence of relative dispersion statistics in isotropic turbulence,” *Physics of Fluids* **20**, 065111 (2008).
- [13] P. Yeung and S. B. Pope, “An algorithm for tracking fluid particles in numerical simulations of homogeneous turbulence,” *J. Comp. Phys.* **79**, 373 (1988).
- [14] R. Benzi, L. Biferale, R. Fisher, D. Q. Lamb, and F. Toschi, “Inertial range eulerian and lagrangian statistics from numerical simulations of isotropic turbulence,” *Journal of Fluid*

Mechanics **653**, 221 (2010).

- [15] R. Benzi, S. Ciliberto, R. Tripiccone, C. Baudet, F. Massaioli, and S. Succi, “Extended self-similarity in turbulent flows,” *Physical review E* **48**, R29 (1993).